

Results of POLDER in-flight absolute calibration

O. HAGOLLE¹, P. GOLOUB², P.Y. DESCHAMPS², T.BAILLEUL², J.M.NICOLAS²,
Y.FOUQUART², A.MEYGRET¹, J.L. DEUZE², M. HERMAN², F. PAROL², F.M.BREON³

1. Centre National d'Etudes Spatiales (CNES)

18,avenue Edouard Belin - 31055 Toulouse CEDEX-France - Olivier.Hagolle@cnes.fr

2. Université des Sciences et Technologies de Lille - Laboratoire d'Optique Atmosphérique

3. Laboratoire de Modélisation du Climat et de l'Environnement - CEA

ABSTRACT

POLDER is a CNES instrument on-board ADEOS polar orbiting satellite, which was successfully launched in august 1996. In november 1996, POLDER entered its nominal acquisition phase and fonctionned perfectly until ADEOS early end of service in june 1997. POLDER is a multispectral imaging radiometer/polarimeter designed to collect global and repetitive observations of the solar radiation reflected by the Earth/Atmosphere System, with a wide field of view (2400 km) and a moderate geometric resolution (6km). The instrument concept is based on telecentric optics, on a rotating wheel carrying 15 spectral filters and polarisers, and on a bidimensionnal CCD detector array. In addition to the classical measurement and mapping characteristics of a narrow-band imaging radiometer, POLDER has a unique ability to measure polarised reflectances using three polarizers (for three of its eight spectral bands, 443 to 910 nm), and to observe target reflectances from 13 different viewing directions during a single satellite pass.

One of POLDER original features is that its in-flight radiometrical calibration does not rely on any on-board device. Many calibration methods using well-characterized calibration targets have been developped to achieve a very high calibration accuracy. This paper presents the various methods involved in the absolute in-flight calibration plan and the results obtained during the calibration phase of the instrument : absolute calibration over molecular scattering, inter-band calibration over sunglint and clouds, inter-calibration with OCTS, water vapor channels calibration over sunglint using meteorological analysis. A brief description of the algorithm and of the performances of each method is given.

1. INTRODUCTION

Radiometrical calibration accuracy is one of the major elements contributing to the quality of the measurements obtained with optical remote sensing instruments. This radiometrical calibration can be achieved through pre-flight measurements in optical laboratories, but these measurements do not always have the required accuracy, and the instruments are subject to degradation after launch because of the aging of the optics or of the outgassing which occurs when the instrument leaves the atmosphere. To cope with this problem, many spaceborne instruments are equipped with on-board calibration devices. SPOT satellites¹⁰ have an inner lamp and an optical fiber system to observe the sun. Actually, the inner lamp is used only for multi-temporal monitoring of the sensitivity of the instruments and for detector normalization, and the solar observations are affected by a difficult pre-flight calibration of the system itself and by a slow degradation of the optical fibers. SPOT calibration relies now mainly on natural targets calibration. OCTS onboard ADEOS is also equipped with inner lamps and a solar observation system, but their use for estimating OCTS calibration is not very accurate because of degradation of the lamps after the launch and because of non-uniformities in the mirror which allows observation of the sun. These problems lead to the decision of using natural targets for OCTS calibration¹⁹. Many future instruments have also based their calibration mainly on on-board devices, such as SeaWIFS, MODIS and MISR on-board of EOS AM-1, but are also developing vicarious methods in order to verify the on-board devices¹⁷.

POLDER project team decided to avoid the developpment of an onboard calibration system. Past experiences of on-board calibration devices in CNES with SPOT satellites have failed to provide accurate results and vicarious methods using natural targets were necessary to obtain the required absolute calibration. Moreover, the implementation of a calibration system in POLDER compact design would have been expensive and hazardous in case of failure, and no device could have covered the entire POLDER bidimensionnal field of view. In order to compensate for the lack of an onboard calibrating source, lots of efforts have been invested in the developpment of a very stable instrument¹ (no variation when passing from air to void), in an exhaustive and accurate pre-flight calibration², and in the adaptation and enhancement of calibration methods over natural targets.

Such methods have been intensively used for the calibration of AVHRR/NOAA or METEOSAT and have achieved good results^{15,16} using natural targets such as molecular scattering over ocean for absolute calibration, high clouds or ocean sun glint for interband calibration and desert sites. POLDER calibration plan makes use of all these methods after some adaptations to make use of the multidirectional and polarisation measurements of the instrument. New calibration methods have also been introduced to characterize POLDER sensitivity to polarisation.

2. THE POLDER INSTRUMENT ON ADEOS

The POLDER radiometer design consists of three principal components: a CCD matrix detector, a rotating wheel carrying the polarizers and spectral filters, and a wide field of view (FOV) telecentric optics (Deschamps et al., 1995). The optics have a focal length of 3.57 mm, opening to f:4.5 with a maximum FOV of 114°.

The CCD sensor array is composed of 242 x 274 independent sensitive areas. The total array detection unit size is 6.5 x 8.8 mm which corresponds to along-track and cross-track FOVs of $\pm 43^\circ$ and $\pm 51^\circ$, respectively, and to a diagonal FOV of $\pm 57^\circ$. The spectral sensitivity of the CCD array extends between 400 and 1050 nm.

The rotating wheel, which has a steady period of 4.9 s, supports the interference filters and polarizers that select the spectral bands and polarisation directions. It carries 16 slots, one of which is an opaque filter to estimate the CCD detector dark current. The remaining 15 slots carry 6 unpolarised and 9 polarised filters (3 polarisation directions for 3 different wavelengths). Thus, POLDER acquires measurements in 9 bands, 3 of which are polarised. POLDER filters have been designed to avoid any spectral variation of the filters when passing from air to void during the launch (filters are made with a Ion Assisted Deposition technology). This characteristic is the key for an accurate in-flight calibration, since the spectral sensitivity of the spectral bands measured before launch is still reliable after launch.

2.1 Spectral bands

POLDER has 15 spectral bands which range from 443 nm to 910 nm. Two of these spectral bands are centered on molecular absorption bands : 763 (O₂) and 910 (H₂O).

POLDER band	443P	443NP	490NP	565NP	670P	763NP	765NP	910NP	865P
Central Wavelength	444.5	444.9	492.2	564.5	670.2	763.3	763.1	907.7	860.8
Approximate Band Width	20	20	20	20	20	10	40	20	40
Polarisation	Yes	No	No	No	Yes	No	No	No	Yes
Saturation level	1.1	0.97	0.75	0.48	1.1	1.1	1.1	1.1	1.1

Table 1 provides the spectral band characteristics for the POLDER instrument aboard the ADEOS-1 satellite. The 9 bands are defined by their central wavelength, spectral width and polarisation capabilities. The saturation levels are given in unit of normalised radiance, i.e. the maximum spectral radiance divided by the solar spectral irradiance at nadir and multiplied by $\cos(\theta_s)$. The dynamic reflectance range is subsequently obtained by dividing the range given in Table 1 by $\cos(\theta_s)$, where θ_s is the solar zenith angle.

Owing to the signal to noise requirements for ocean colour measurements, the 443 nm channel had to be split into a polarised band (3 filters: 443P) and an unpolarised band (1 filter: 443NP).

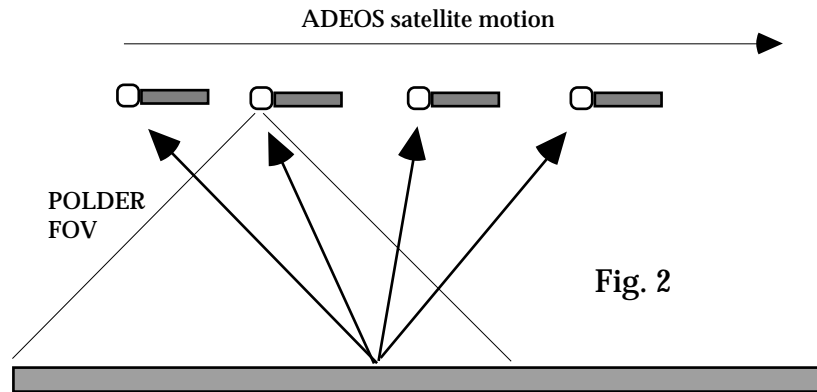
2.2. Polarisation measurements

For three of the eight spectral bands (443, 670 and 865 nm), a polariser is added to the filters in order to assess the degree of linear polarisation and the polarisation direction. These parameters are derived by combining measurements in three channels with the same spectral filters but with the polariser axes turned by steps of 60°. The three polarisation measurements in a spectral band are successive and have a total time lag of 0.6 s between the first and the third (last) measurement. In order to compensate for spacecraft motion during the lag and to register the three measurements, a small-angle, wedge prism is used in each polarising assembly. As a consequence, the matrix image is translated in the focal plane to offset the satellite motion, and the three polarisation measurements are quasi collocated.

2.3. Spatial resolution

The ground size or resolution of a POLDER-measured pixel from ADEOS is $6 \times 7 \text{ km}^2$ at nadir. Due to the earth curvature, there is a slight viewing angle dependence of the pixel size, leading to an increase of 21% for an incidence angle of 60° .

2.4. Data acquisition



The POLDER instrument is in imaging mode on the sunlit part of the ADEOS orbit only. Data acquisition starts when the solar zenith angle on the Earth surface at the satellite nadir is smaller than 75° and stops, in the South, when it is larger than 75° . The 16 filter sequence is repeated every 19.6 s. During this interval, a given point on the surface, initially at nadir viewing, moves by about 9° relative to the satellite (Fig. 2). The point remains within the POLDER field of view. As the satellite passes over a target, about 12 (up to 14) directional radiance measurements (for each spectral band) are performed aiming at the point (Figure 3). Therefore, POLDER successive observations allow the measurement of the bidirectional reflectance properties of any target within the instrument swath.

3. POLDER RADIOMETRIC MODEL

3.1. Presentation

The objective of the radiometric model of the instrument is to give a synthetic but totally representative description of the physics of the instrument in order to characterize the response to any input polarized light for each pixel of the detector matrix, in each spectral channel.

3.2. Stokes parameters :

Multiple, as opposed to single, scattering/reflection processes induce elliptic polarization. Radiative transfer simulations show that the fourth component of the Stokes vector of top of the atmosphere (TOA) light is negligible compared to the others. This means that the polarization is mostly linear for prevailing atmospheric conditions. Consequently, the POLDER instrument senses only the linearly polarized Earth-reflected radiance. Thus, the light received by POLDER can be expressed with only three parameters : intensity of the light I , polarization rate P and polarization direction θ . In order to avoid trigonometric functions in the formulas and to allow the use of a matricial formalism, we use the Stokes parameters I , Q , U .

I : normalized total radiance = $\frac{\text{radiance}}{\text{Solar flux}}$

$$Q = I.P \cos 2\theta$$

$$U = I.P \sin 2\theta$$

In the following sections, Q and U are always expressed in a coordinate system such that $U=0$ when the light is polarized in the radial direction (this coordinate system is different for every (l,p) detector and is referred to as beam coordinate system). According to the Fresnel-Descartes laws, the unwanted polarization effect of the optics is only sensitive to the Q component of the Stokes vector.

3.3 Radiometric model

For the non-polarized channels, the radiometric model is written :

$$X_{lp}^{mk} = G^m \cdot A^k \cdot p^k(\theta) \cdot g_{lp}^k \cdot (I_{lp}^k + k(\theta) \cdot Q_{lp}^k) \quad (1)$$

where :

l : line number in the CCD matrix (1 ≤ l ≤ 242),

p : column number in the CCD matrix (1 ≤ p ≤ 274),

m : electronic amplification factor number (1 ≤ m ≤ 7),

k : spectral band number (0 ≤ k ≤ 9),

X_{lp}^{mk} : digital count measured by the pixel (0 ≤ X_{lp}^{mk} ≤ 4095),

I_{lp}^k : normalized radiance observed by (l,p)

Q_{lp}^k : second component of Stokes vector (normalized radiance) observed by (l,p)

G^m : electronic amplification factor ($G^6 = 1$),

A^k : absolute calibration coefficient

$p^k(\theta)$ expresses the low frequency variations of the optic transmission which decreases a little when the viewing angle increases.

$k(\theta)$ expresses the optics polarization rate which leads to unwanted sensor sensitivity to polarized light. $k(\theta) = 0$ at the array centre and increases up to 3% in the corners of the CCD array.

g_{lp}^k : refers to high frequency variations of the sensitivity of the elementary detectors, mainly linked to non-homogeneities in the CCD matrix, but also eventually to the presence of a few dust particles on the optics.

The model makes a distinction between the high and low frequency relative transmission in order to be in compliance with the in-flight calibration methods which are different for the 2 parameters.

INCORPORER "ExcelChart" * mergeformat



Figure 3 : Typical response on a radial section of the CCD ($p^k \cdot g_{lp}^k$) for a non polarized band. The smooth line represents the low frequency variation p^k .

For the polarized channels, the radiometric model is written :

$$X_{lp}^{mka} = G^m \cdot A^k \cdot T^{ka} \cdot p^k() \cdot g_{lp}^{ka} (P_1^{ka} \cdot I_{lp}^k + P_2^{ka} \cdot Q_{lp}^k \cdot P_3^{ka} \cdot U_{lp}^k) \quad (2)$$

where the new terms are :

a : polarized channel number (1, 2, 3),

T^{ka} : relative calibration coefficient of polarisers,

$P_1^{ka}, P_2^{ka}, P_3^{ka}$ express the effect of the polarizers and of the optics polarization rate on the Stokes vector.

These parameters can be expressed in the Local Coodinate System as follows :

$$P_1^{ka} = 1 + k() \cdot k \cos 2(- ka)$$

$$P_2^{ka} = k() + k \cos 2(- ka)$$

$$P_3^{ka} = k \sin 2(- ka)$$

is the efficiency of the polarizers ($1 < < 0.98$)

ka is the polarization angle of the polarizers ($-60^\circ, 0, 60^\circ$)

Combining the three equations of the radiometric models for the three polarized channels of the same spectral band, this model can be written under a matricial formalism that is used to compute the Stokes parameters :

$$\begin{pmatrix} X_{lp}^{k1} \\ X_{lp}^{k2} \\ X_{lp}^{k3} \end{pmatrix} = G^m A^k p^k() \begin{pmatrix} T^{k1} g_{lp}^{k1} P_1^{k1} & T^{k1} g_{lp}^{k1} P_2^{k1} & T^{k1} g_{lp}^{k1} P_3^{k1} \\ T^{k2} g_{lp}^{k2} P_1^{k2} & T^{k2} g_{lp}^{k2} P_2^{k2} & T^{k2} g_{lp}^{k2} P_3^{k2} \\ T^{k3} g_{lp}^{k3} P_1^{k3} & T^{k3} g_{lp}^{k3} P_2^{k3} & T^{k3} g_{lp}^{k3} P_3^{k3} \end{pmatrix} \begin{pmatrix} I_{lp}^k \\ Q_{lp}^k \\ U_{lp}^k \end{pmatrix} \quad (3)$$

3.4 Pre-flight Calibration

POLDER instrumental concept on-ground calibration gives rise to two main difficulties : the necessity (1) to calibrate a bidimensionnal very wide field of view, and (2) to characterize perfectly the polarization sensitivity in the whole field of view. The pre-flight accuracy relied on an important hardware composed of :

- two integrating spheres : a large integrating sphere for the calibration measurements and a transfer integrating sphere in order to check the air/vacuum stability of the absolute calibration, to control the stability of the reference radiometer and to determine the large integrating sphere non uniformities.

- a polarizing system which enables to generate different polarization rates and directions. It is made up of two parallel glass plates which can be orientated around two axes.

- a reference radiometer fitted with filters which are identical to POLDER ones. The radiometer is used for absolute calibration and has been calibrated with each of the filters in L.C.I.E. (Laboratoire Central des Industries Electriques). This calibration has been operated against a spectrally calibrated source which is a standard incandescent lamp and a BaSO₄ plate to have a good uniformity, and a standard radiometer. The estimated accuracy of this calibration is $\pm 3.5 \%$.

- a monochromator to measure the spectral response of the instrument ; the rotation of the grating is synchronous with the instrument imaging cycle and the emission stability of the lamp is checked all along the measurement. The stability of the response over several measurements is better than 1 % and the variation of the centering of the spectral profile is less than 0.3 nm.

The evaluated accuracies on the parameters of the radiometric model are presented in the table 4. Absolute calibration and thus spectral responses of the filters did not vary when measurements were made in a vacuum chamber.

G^m	A^k	$T^{k,a}$	$g_{l,p}^k$	$p^k.p_1^k$	$p^k.p_2^k$	$p^k.p_3^k$
$\pm 0.1 \%$	$\pm 5 \%$	$\pm 0.1 \%$	$\pm 0.1 \%$	$\pm 1 \%$	$\pm 1 \%$	$\pm 1 \%$

Table 4 : Evaluated accuracies for the determination of the radiometric model parameters

4. IN-FLIGHT RADIOMETRICAL CALIBRATION

In order to ensure good in-flight radiometrical performances, each calibration parameter of the radiometrical model can be measured and monitored using various in-flight calibration methods (except for the polarisers direction coefficients (k_a). Absolute calibration methods aim to measure the A^k parameter, relative calibration methods measure the $p^k(\)$ and g^{ka}_{lp} parameters, and polarisation calibration methods deal with k and $k(\)$. POLDER relative calibration results are reported in the same conference¹⁸, and polarisation calibration methods were presented elsewhere¹⁵. This paper deals with absolute calibration

POLDER absolute calibration is achieved through an absolute calibration of the "blue" spectral bands (443P, 443, 490 and 565) using the well-characterized Rayleigh scattering over ocean. This absolute calibration is then transferred to the other wavelengths through inter-band calibration using the specular reflection of the sun over the ocean. These two nominal methods can be validated using inter-band calibration over clouds, cross calibration with OCTS (Ocean Color and Temperature Scanner) on board of ADEOS, absolute calibration using the polarised part of Rayleigh scattering, and multi-temporal calibration over desert sites.

4.1. Absolute calibration over Rayleigh Scattering

Rayleigh (or molecular) scattering over ocean is a well-characterized target in the blue spectral range (443P to 565 spectral bands). For a given angular condition the main variability sources of the signal are water leaving radiance, foam and aerosols but they can be reduced through a strict selection of the pixels used for calibration. Calibration points are selected among POLDER data according to criteria defined to minimize the non-molecular contribution to the measured signal. They are chosen inside geographic areas having an a priori wellknown weak and stable chlorophyll content, with no clouds, a low wind speed, and a low aerosol optical thickness. These areas are located using POLDER ocean color synthesis and the associated water reflectance is estimated using Morel model¹¹.

Two "extreme" chlorophyll contents are systematically considered: 0.035mg.m^{-3} and 0.17mg.m^{-3} for these areas. Cloudy pixels are eliminated using a cloud screening based on the 865 nm radiance and meteorological data (ECMWF) are used to select zones with a low wind speed ($< 5 \text{ m.s}^{-1}$). The aerosol content is estimated using the channel 865nm and observations with a normalized radiance under 0.002 are selected (after subtraction of rayleigh scattering contribution) which corresponds to an optical thickness under 0.05.

Our calibration method is derived from¹⁴. The pre-flight/in-flight variation of the calibration coefficient is obtained through the formula :

$$A^k = \frac{A^k_{\text{in-flight}}}{A^k_{\text{pre-flight}}} = \frac{MI^{k,oz}}{CI^k(v_w) + I^{k,865} \cdot (MI^{865} - CI^{865}(v_w))}$$

where :

- $MI^{k,OZ}$ is the normalized radiance measured by POLDER (with pre-flight calibration) in a band k among { 443P,443,490,565 } This radiance has been corrected for ozone absorption which is derived from Total Ozone Monitoring Scanner (TOMS) which was also on-board ADEOS.

- CI^{k,v_w} is the computed molecular scattering radiance over ocean which is a function of geometrical conditions, chlorophyll content and wind speed v_w obtained from meteorological data (ECMWF). The look up tables are obtained with a Successive Orders of Scattering (SOS) code⁴.

- $I^{k,865}$ is also a look up table as a function of the viewing geometry, and derives the aerosol contribution on the signal in spectral band k from the optical depth measured in the 865 nm spectral band. Computations are performed with (SOS) for two tropospheric aerosol models¹³ : a coastal model with 70% humidity and a marine model with 98% humidity.

A calibration result is the average of the calibration coefficients obtained during a five day period using one of the two chlorophyll content and one of the two aerosol models ; it is thus based on more than 20000 calibration points. Calibration coefficients (table 5) have been measured for the 4 channels over 3 periods of 5 days, leading to twelve calibration results. The $Ak(\text{in-flight})/Ak(\text{preflight})$ value is the mean value of these results, and the maximal dispersion is the maximum difference between the mean value and each of the twelve results. This methods makes use of the 865 nm spectral band which must be well calibrated. This implies iterations with sunglint calibration method described below. The results are given after two iterations with the sunglint calibration method.

Spectral band	443P	443	490	565
$Ak(\text{in-flight})/Ak(\text{preflight})$	0.975	0.965	0.995	1.035
Maximal dispersion (%)	3.5	3.5	1.9	2.3

Table 5 :Results of POLDER absolute calibration over rayleigh scattering

A detailed analysis shows that channels 443 and 565 are quite sensitive to water color (up to 2% for 443), while channel 490 sensitivity to this parameter is rather small (0.6%); this is because of the low water reflectance variation as a function of the chlorophyll content around 500nm. Channels 490 and 565 are more sensitive (up to 1%).to the aerosol model because the molecular scattering decreases faster than aerosols contribution when the wavelength increases. Finally calibration coefficients strongly depend on the scattering angle (up to 1.5%) which means that some directionnal effects are not perfectly modelized such as water leaving radiance which is supposed to be lambertian.

4.2. Inter-band calibration over sunglint

This method uses the specular reflection of the sun on the sea surface. Specular reflection is known to be spectrally flat and has a high radiance which limits the influence of other error sources such as water leaving radiance or aerosols. Sunglint radiance depends only on the wind speed and is determined using 565 nm measurement. This is used to calibrate 670, 765 and 865 spectral bands. The calibration of 763 and 910 nm channels requires ancillary information to evaluate the high atmospheric absorption : surface pressure (for 763) and atmospheric water vapor content (for 910) derived from ECMWF analysis.

The algorithm is as follows : to begin, all radiances are corrected from molecular absorption. Ozone absorption is derived from TOMS. Oxygen absorption in 765 spectral band is corrected using 763 nm measurement. Water vapor amount is determined using POLDER 865 nm and 910 nm measurements (ECMWF data are used only for 910 calibration). A first guess of the calibration factor is derived by neglecting the aerosol influence. Given the measurement in the calibrated channel (here 565 nm), an estimate of the sea surface roughness can be deduced, which allows to estimate the absolute radiance in the other channels. This step needs only interpolations within a pre-calculated look up table computed though a Successive Orders of Scattering code⁴.

Then, these approximate results are corrected from the aerosol effect. This correction uses one of POLDER properties which is to be able to look at the same point from different angles in the same orbit. It is thus possible to find a direction which is out of the sunglint direction. The correction is based on the correlation between the error resulting from the aerosol effect in the specular direction and the measurements in off sunglint directions, which are informative about the aerosol properties.

From numerical simulations of the radiance at the Top of the Atmosphere for a large set of aerosol models, the correction is derived statistically in a polynomial form of the estimated absolute normalized radiance and of the normalized radiances observed at 670 and 865 nm in a direction off sunglint.

To select the calibration points suitable to this method, an important criterion has been added to the criteria involved in the molecular scattering method. The viewing direction of the calibration point must be within a cone of 6 degrees centered on the exact specular direction ($\theta_s = \theta_v, \phi_s = \phi_v + 180^\circ$). For higher values, the dispersion of the results increases quickly, indicating that the geometrical modelization of the sunglint is less accurate and its relative contribution is smaller. The off-sunglint 865 maximal radiance threshold is a little higher than for calibration over molecular scattering, and has been set to 0.005 in normalized radiance units.

The accuracy of the intercalibration scheme is principally limited by two factors:

- the error on the absolute calibration of the reference channel, that is reported in all other channels with a slight amplification.
- and the error on the aerosol correction, which results from the calibration uncertainties in the near infrared channels 670 and 865 nm.

A calibration result is the average of the calibration coefficients obtained during a five day period, ie more than 2000 calibration points. Calibration coefficients (table 1) have been measured for the 5 channels over 5 periods of 5 days. The

A_k value is the mean value of these elementary results, and the maximal dispersion is the maximum difference between the results obtained for each of the five periods. The results given in table 6 were obtained after having calibrated the 565 reference band over rayleigh scattering.

Spectral band	670P	763	765	865	910
Ak(in-flight)/Ak(preflight)	1.03	1.023	1.037	1.05	1.027
Maximal dispersion (%)	0.9	0.9	1.2	1.4	3.5

Table 6 :Results of POLDER inter-band calibration over sunglint

A full analysis of the elementary measurements does not show any significant dependency of all the results on any of the algorithm parameters. For example, we did not detect any correlation between the measured calibration coefficient and the aerosol optical thickness, indicating that the aerosol scattering has been properly corrected. Some correlation was found, however, between A865 and the atmospheric water vapour amount when H2O absorption, which included a modelisation of the continuum absorption was applied in the process. We therefore decided to account only for the line absorption and the correlation disappeared.

The results obtained for the 910 nm spectral band show a rather high dispersion which comes from the limited accuracy of the water vapor information contained in weather analysis data. The results obtained in the other spectral bands are excellent and a great confidence can be given to this calibration method.

The same calibration method can be applied using 443P instead of 565 as reference. This leads to degraded calibration performance because of water leaving radiances uncertainties and because of the higher spectral distance between 443P and the near infrared spectral bands. However this method enabled us to verify 443P/565 intercalibration with an independent method. If we suppose $A_k(565) = 1.035$ (as obtained with rayleigh scattering method), then the intercalibration gives 0.97 for 443P, very close from 0.975 obtained with rayleigh scattering method.

4.3. Inter-band calibration over clouds

Clouds are white and bright sources, and therefore are good targets for interband calibration. However, their spectral signature depends a little on their optical depth, on their altitude (because of the above atmosphere), on the surface below (because of the cloud transparency), on the angular conditions of observation, and also on the type and size of water or ice particles. Cloudy calibration points are thus carefully selected according to the following criteria : clouds over sea, very high reflectance (above 0.8) to minimize underlying surface effects, high cloud altitude (derived from O2 pressure) in order to minimize aerosol effects and select only clouds with ice particles, close to vertical viewing angle. After correction for ozone

absorption, the inter-band ratio obtained with POLDER measurements are compared to simulations made with different types of ice particles.

For the results given below, 670 nm spectral band was used as a reference to derive 443 and 865 absolute calibration coefficients :

Spectral band	443P	670	865
Ak(in-flight)/Ak(preflight)	1.02	1.03	1.02

Table 7 : Results of POLDER inter-band calibration over clouds

The results of this method disagree for 443P band with the results of the other methods but no explanation has yet been found for this discrepancy.

4.4. Cross calibration between POLDER and OCTS

Simultaneous acquisitions of POLDER and OCTS data have been used in order to cross calibrate both sensors. Since the two sensors are on the same platform and share 6 spectral bands, it is possible to compare the radiances of targets observed at the same time, with the same viewing and solar angles and in nearly identical spectral bands. In order to enhance the accuracy of the method, the targets are chosen so that they have a high normalized radiance (more than 0.2), a low polarization rate, and a good spatial uniformity to discard possible registration errors between the two sensors. The targets corresponding to these criteria are mostly clouds.

Table 8 gives the percent difference in the radiances measured by POLDER and OCTS using the most up-to-date calibration values (ie POLDER in-flight calibration obtained with molecular scattering and sunglint methods, and OCTS in-flight vicarious calibration). A positive value indicates that OCTS measurements are higher than POLDER's.

Spectral band	443	490	565	670	765	865
I (%)	1.2	5.5	-2.9	1.2	1.3	8.6

Table 8 : Results of POLDER-OCTS cross- calibration

Apart from the 865 nm result, these results confirm that the radiances observed by the two sensors are very close and therefore give more confidence to both sensors calibration. 865 nm rather bad result may be related to OCTS vicarious calibration over ocean, because of the very low signal in this band. At the time when this paper was written, no other OCTS calibration result was available for this spectral band, although new ones should be released in september 97.

5. CONCLUSION

A new calibration approach has been developed at CNES for POLDER, based on the design of a very stable instrument, on an exhaustive calibration of the instrument and on the development of many in-flight operational calibration methods using natural targets. The obtained results are very satisfactory since the in-flight absolute calibration has shown that :

- POLDER instrument is stable : all in-flight absolute calibration coefficients differ from pre-flight coefficients by less than 5%.
- all in-flight calibration methods agree within a margin of 3% (except for interband calibration over clouds with 443P)

The overall accuracy of POLDER in-flight calibration is estimated to be better than 3-4% and the new coefficients have been introduced in POLDER level 1 products. This accuracy has also been validated through inter-calibration with OCTS which was calibrated independently using a different radiative transfer code. Such an accuracy could not have been achieved without a good characterisation of POLDER polarisation sensitivity since all our calibration sources are very polarised. Still some uncertainty exists in the absolute calibration of the 443 nm channels and our work is ongoing to reach the challenging objective of 2-3% absolute calibration.

In-situ water leaving radiance and aerosols optical depth measurements are currently being processed to verify Rayleigh scattering results. Research is also beginning to develop a new Rayleigh scattering calibration algorithm which uses POLDER multidirectional properties to derive at the same time absolute calibration and water leaving radiances.

6. REFERENCES

1. Andre, Y., JM.Laherrere, T.Bret-Dibat, M.Jouret, JM.Martinuzzi, and J.Perbos; 1995: Instrumental concept and performances of the POLDER instrument: SPIE proceedings Infrared spaceborne remote sensing III, Vol 2553, San Diego, July 95
2. Bret-Dibat, T., Y. Andre, JM.Laherrere; 1995: Preflight calibration of the POLDER instrument. SPIE proceedings Remote Sensing and reconstruction for three Dimensional Objects and Scenes, Vol 2572, San Diego, July 95
3. Deschamps, P.Y., F.M. Bréon, M. Leroy, A. Podaire, A. Bricaud, J.C. Buriez, and G. Sèze; 1994: The POLDER Mission: Instrument Characteristics and Scientific Objectives. IEEE Trans. Geosc. Rem. Sens. **32**, 598-615.
4. Deuzé, J.L., Herman M., and Santer R., Fourier series expansion of the transfert equation in the atmosphere ocean system, J. Quant. Spectr. Rad. Transfert, 41, 483-494, 1989.
5. Goloub, P., B.Toubbe, M. Herman, T.Bailleul, O.Hagolle, J.M.Martinuzzi, B.Rougé, In-flight Polarization Calibration of POLDER, Proc of the EUROPTO Advanced and Next-Generation Satellites, vol 2957, pp. 299-310, 1996
6. Hagolle, O., A. Guerry, L. Cunin, B. Millet, J. Perbos, J-M. Laherrere, T. Bret-Dibat and L. Poutier : POLDER Level 1 Processing Algorithms. Spie Aerosense 96, Proceedings : "Algorithms For Multispectral And Hyperspectral Imagery II" Orlando, 308-319, 1996
7. Holben, B.N., Y.J. Kaufman and J.D. Kendall, 1990. NOAA_11 AVHRR visible and near-infrared in-flight calibration. Int. J. Remote Sensing 11,1511-1519.
8. Koepke P. "Effective reflectance of oceanic white caps" (1984), Applied Optics, 20, 34.
9. Lifermann, A., J.L. Counil, J.M. Martinuzzi, and J. Perbos; 1995: General outlines of the POLDER experiment : Symposium "Satellite Remote Sensing II", Septembre 1995, Paris, France. SPIE proceedings, pp 245-252.
10. Meygret, A., O. Hagolle, P. Henry, M. Dinguirard, P. Hazane, R.Santer and J.L. Deuzé,1994. SPOT 3 : first in-flight calibration results. Proceedings : IGARSS'94 Pasadena.
11. Morel A., "Optical modeling of the Upper Ocean in Relation to its Biogenous Matter Content (Case I Waters), Journal of Geophysical research, volume 93 number C9 page 10,749-10,768 (september 15th 1988).
12. Sakuma, F., T.Bret-Dibat, H.Sakate, A.Ono, J.Perbos, JM.Martinuzzi, K.Imaoka, H.Oaku, T.Moriyama, Y.Miyachi, and Y.Tange; 1995: POLDER-OCTS preflight cross calibration using round robin radiometers: , SPIE proceedings Infrared spaceborne remote sensing III, Vol 2553, San Diego, July 95
13. Shettle E., Fenn R., "Models for the Aerosols of the Lower Atmosphere and the Effects of Humidity Variations on Their Optical Properties.",AGFL-TR-79-0214, September 20th, 1979.
14. Vermote, E., R.Santer, P.Y. Deschamps and M.Herman : 1992. In-flight calibration of large field of view sensors at short wavelengths using Rayleigh Scattering. International journal of Remote Sensing, Vol 13, N°18 ; pp 3409-3429
15. Vermote, E. and Y.J. Kaufman, 1995. Absolute calibration of AVHRR visible and near infrared using ocean and cloud views. International Journal of Remote Sensing, Vol 16, N013, pp 2317-2340.
16. Kaufman, Y.J and B.N. Holben, 1993, Calibration of the AVHRR visible and near-infrared bands by atmospheric scattering, ocean glint and desert reflection. International journal of remote sensing, 14, 21-52.
17. Slater P.N., Biggar S.F., Thome K.J., Gellman D.I., Spyak P.R., 1996, Vicarious Radiometric Calibrations of EOS sensors, American Meteorological Society Journal
18. Cosnefroy H., X. Briottet, P. Soule, O. Hagolle, F. Cabot, 1997, POLDER multi-angular calibration using desert sites : method and performances. proc of Aerospace remote sensing
19. H. Oaku, 1997 : OCTS calibration, proc of The Second ADEOS Symposium/Workshop, Yokohama, pp 161-173